



Sharif University of Technology

Scientia Iranica

Transactions F: Nanotechnology

www.scientiairanica.com



# Numerical study of mixing enhancement through nanomixers using the throttling approach

M. Darbandi<sup>a,b,\*</sup> and M. Sabouri<sup>a</sup>

a. Department of Aerospace Engineering, Centre of Excellence in Aerospace Systems, Sharif University of Technology, Tehran, Iran.

b. Institute for Nanoscience and Nanotechnology, Sharif University of Technology, Tehran, Iran.

Received 6 September 2014; received in revised form 8 January 2015; accepted 13 April 2015

## KEYWORDS

Nanomixer;  
Throttling;  
Mixing length;  
Mixing flow rate;  
DSMC method.

**Abstract.** In this study, we intend to improve the mixing performance of a nanoscale mixer using the throttling idea. The study is conducted at a Knudsen number of 0.12, which corresponds to the transitional flow regime. Therefore, we have chosen the DSMC method to perform reliable numerical simulations. We consider a number of different throttles with various widths and shapes to enrich our study and to explore a wider range of their influences on the mixing evolution. We choose a linear converging-diverging nozzle profile, an arced converging-diverging nozzle profile, and a sudden contraction-expansion configuration as our throttle shapes. The results show that both the mixing length and the mass flow rate decrease as the throttle widths decrease. However, the decrease in throttle width plays a more effective role in reducing the mixing length than the decrease in mass flow rate. Evaluating the results of three chosen throttle shapes, we conclude that the arced nozzle and sudden contraction-expansion shapes result in less mixing length and mass flow rate magnitudes; although the reductions are more pronounced for the latter shape. We also conclude that throttle shape affects the reduction in mixing length more seriously than the reduction in mass flow rate.

© 2015 Sharif University of Technology. All rights reserved.

## 1. Introduction

For many years, micro/nanofluidic devices have received much attention due to their several benefits. These small length and time scale devices occupy small spaces, handle very small fluid quantities, consume little energy, and provide fast and accurate responses. Today, there are many different types of micro/nanofluidic device of which a few may utilize very small gas mixers mostly to provide suitable environments for proper chemical reactions. Microscale reactors [1] and power-generation systems [2] are examples of such systems in which a complete and fast mixing is targeted to improve the overall efficiency of the device.

Therefore, it is necessary to study the possible parameters, which can improve the mixing efficiency of such micro/nanomixers and can lead to a superior design for these devices. Indeed, further size reduction promotes researchers to expand their studies to include nanoscale mixers.

As is known, the flow through micro/nanofluidic devices is laminar. As a result, the mixing relies solely on molecular diffusion. Therefore, manipulating the parameters affecting molecular diffusion is the only way to enhance the mixing in such small length scales. These parameters mostly include the fluid molecular diffusion coefficient, the interfacial area between the two mixing fluids, and the species concentration gradients. Regarding the molecular diffusion coefficient parameter, we know that increasing the fluid temperature will readily enhance the mixing; see Refs. [3,4]. Therefore, the primary idea behind the mixing en-

\*. Corresponding author. Tel.: +98 21 66164644;

Fax: +98 21 66022731

E-mail address: darbandi@sharif.edu (M. Darbandi)

hancement is clear for this case. However, the two other parameters depend on mixer geometry. Therefore, some mixing enhancement strategies, such as multi-lamination [5,6], splitting and recombination [7,8], and chaotic advection [9,10], have been already suggested to increase either the available interfacial area or the concentration gradient magnitudes.

An alternative idea for increasing species concentration gradients, without benefiting from very complex geometries, is to place a throttle or contraction shape in the passage of mixing [11–15]. These shapes are also referred to as a contraction-expansion arrangement [14]. These configurations locally reduce the width of the mixing passage. Therefore, comparing with the case in which the entire width of mixing passage is reduced, these local reductions would reduce the pressure drop at a fixed flow rate or would decrease the flow rate at a fixed pressure drop. Although the contraction-expansion arrangements would generate desirable recirculation zones behind them [13–15], this would not be a benefit for nanomixers because of working with very low Reynolds number flows. The literature on micromixers shows that placing obstructions in the flow passage can also lead to mixing enhancement in them, similar to using contraction-expansion in the flow passage [16–18].

A careful review on micromixer literature shows that past numerical studies have been mostly focused on liquid stream mixing. Roughly, there are much fewer publications addressing gas-gas mixing [3,4,9,12,19–25]. Additionally, these gas-gas mixing studies are mostly limited to continuum or early slip flow regimes [9,12,19–21,23,25]. This is why such works could readily use the continuum-based numerical methods with slight modifications to perform their simulations. Indeed, there are extended continuum-based governing equations, derived from the fundamental gas kinetics theory, which can help to describe multicomponent flows, such as mixing ones [26–29]. Alternatively, one may use slip/jump boundary conditions and incorporate them into the continuum-based governing equations to simulate the slip flow regime for either simple gas [30–35] or gas mixture flows [36,37]. In spite of such available approaches, a special concern remains for the simulation of gas mixture flows in nanoscale. Indeed, an accurate study of gas mixing in transitional flow regimes, which is the case for gas mixing in nanoscale, requires special numerical methods capable of accurate capturing of the rarefaction effects in such length scales. The Direct Simulation Monte Carlo (DSMC) method [38] has been chosen as a very accurate simulation method to study rarefied micro/nanoflows [39–47]. Indeed, there are few studies utilizing the DSMC in order to simulate gas mixing through micro/nanochannel cases [3,4,22,24]. On the other hand, past DSMC references have mostly focused on the effects of operating conditions, such as

the inlet-outlet pressure difference or its resulting main velocity magnitude [3,4,22,24], the pressure ratio of the two incoming streams [22], the temperature of incoming streams or mixer walls [3,4], the accommodation coefficient magnitude for the mixer walls [3,22], the effects of some dimensionless parameters, such as Mach number [3] and Knudsen number [3,4] magnitudes, the effects of geometrical parameters, such as the mixer cross section aspect ratio [4], and the size of a bump placed in the flow passage [24] on the mixing performance of the corresponding mixers.

From another perspective, the above DSMC studies mostly focus on microscale mixers. There has been less attention paid to mixing in channels with submicron widths working in transitional flow regimes. With the fast progress in micro/nano propulsion systems [46,48,49], it has become necessary to investigate the fast mixture of two gases in warm micro/nano propulsion devices. This has promoted the current authors to take one further step and study the gas mixing issue in transitional flow regimes through nanomixers. In the present work, we study the mixing in channels with a maximum width of 400 nm. We intend to extend the idea of using a contraction in the mixing channel of a microscale mixer, e.g. utilizing a rectangular bump [24] into nanoscale mixers, similarly. In this regard, we first study the effects of contraction width on the nanoscale mixer performance utilizing a linear converging-diverging contraction. To expand our study and to evaluate the effects of contraction shape on mixing through nanoscale mixers, we next introduce three different contraction profiles: a linear converging-diverging nozzle, an arced converging-diverging nozzle, and a sudden contraction-expansion shape. To the authors best knowledge, such investigations have not been previously elaborated on for either micro or nanoscale gas mixers. Generally speaking, since our study is performed in the transitional flow regime, the achieved results would be valid only in this flow regime. Evidently, if one wishes to study the effects of throttle size and shape in a wide range of rarefaction levels, one should include the effects of Knudsen number variation in the study. However, this is not a concern in this paper.

## 2. Numerical method

The Boltzmann equation is fundamental in describing the behavior of dilute gases in the whole range of rarefaction. For a mixture of  $S$  species, the Boltzmann equation can be stated for each species as follows [38]:

$$\begin{aligned} \frac{\partial}{\partial t}(n_p f_p) + \mathbf{c}_p \cdot \frac{\partial}{\partial \mathbf{r}}(n_p f_p) + \mathbf{F} \cdot \frac{\partial}{\partial \mathbf{c}}(n_p f_p) \\ = \sum_{q=1}^S \int_{-\infty}^{\infty} \int_0^{4\pi} n_p n_q (f_p^* f_{1q}^* - f_p f_{1q}) c_{r,pq} \sigma_{pq} d\Omega d\mathbf{c}_{1q}, \end{aligned} \quad (1)$$

in which  $n$  is the number density,  $f$  is the velocity distribution function,  $\mathbf{r}$  is the position vector,  $\mathbf{c}$  is the molecular velocity vector,  $\mathbf{F}$  is the external force vector,  $c_r$  is the relative velocity magnitude,  $\sigma$  is the collision cross section, and  $\Omega$  is the solid angle. Subscripts,  $p$  and  $q$ , respectively, denote the values for molecules of types  $p$  and  $q$ . Subscript 1 corresponds to the collision partner, and superscript  $*$  denotes the post-collision values. Moreover, the macroscopic flow properties can be calculated from the moments of velocity distribution function [38]. Basically, because of the numerical difficulties associated with the solution of a Boltzmann equation, there are alternative approaches, such as direct simulation methods, to suitably simulate high Knudsen number micro/nanoflows. Therefore, we use the Direct Simulation Monte Carlo (DSMC) method, as the most known direct molecular method for simulating high Knudsen number gas flows, to perform our study. This method was first developed by G.A. Bird to study rarefied gas dynamics flow problems [38]. However, this method has been widely used to simulate many different micro- and nanoscale flows since then [39–47].

As the first step to the DSMC method, the flow domain needs to be divided into a large number of computational cells. Then, a number of simulated molecules are distributed in each cell, based on an arbitrary initial condition for the macroscopic properties, such as the velocity vector, temperature, and density. Each simulated molecule represents a specific number of real molecules. At each time step, the simulated molecules are moved according to their velocity characteristics. However, appropriate boundary conditions are applied to the molecules, which collide with the boundaries. In fact, these molecules are reflected into the main domain with a velocity determined by using suitable wall reflection models. On the other hand, the molecules exiting the open boundaries are removed from the simulation domain. To maintain the desired stationary flow conditions at the open boundaries, it is necessary to inject new molecules from those boundaries into the domain. After suitable boundary treatments, it is necessary to attribute each molecule to its new cell. Using a stochastic algorithm, the collision partners are determined among the molecules of each cell and then their post-collision velocities are determined based on the chosen appropriate collision model. After taking sufficient time steps in which the effects of initial conditions are eliminated, the sampling should be started. After each certain number of time steps, the microscopic properties of the molecules are sampled in each cell. The macroscopic properties are then calculated by a suitable time-average of collected sampled data. The time step advancement and the sampling procedure are continued until the statistical errors are damped out sufficiently.

In the present work, we use an extended version of

the dsmcFoam simulation code to perform our DSMC simulations [40,42–46,50]. We use the characteristics-based inlet/outlet boundary conditions to simulate the pressure driven flows in this code. The details of such boundary condition treatments have been completely described by Wang and Li [39]. Since the incoming streams at the mixer inlets are simple  $\text{N}_2$  and  $\text{CO}$  gases, there is no need to adapt the inlet pressure boundary condition treatments presented by Ref. [39] in this work. However, the outlet boundary condition treatment needs further care, because the composition of mixed gas may not be either uniform or known a priori. Indeed, the geometries defined in the present work have mixing channels long enough to achieve a complete uniform mixing at the outlet. In other words, we assume there is no more mixture composition variation along the mixer at exit. Therefore, it is reasonable to assume that the mixture composition at the outlet face elements will be the same as the composition in their adjacent cells. The composition in each cell is updated during the simulation until achieving a steady-state value. Knowing the composition magnitudes at the outlet face elements, we apply the outlet boundary treatment suggested by Ref. [39] to the mixture, while the injected molecules are redistributed between the mixture constituents, based on their calculated mole fraction values.

In the present study, the molecule-wall interactions are treated as fully diffuse reflections. The molecular collisions are modelled as Variable Soft Sphere (VSS) collisions, considering the model parameters reported in [38]. The rotational energy redistribution is performed using the Larsen-Borgnakke model with a constant relaxation probability of  $1/5$ .

### 3. DSMC code validation

As elaborated on in Section 2, we developed the current DSMC method gradually and validated its accuracy along its development. For example, we validated our code in treating subsonic flow through micro/nanochannels [40,43,44], subsonic-supersonic flow through micro/nano nozzles [42], flow over micro/nano obstacles [45] and flow through micro/nanoscale hot thrusters [46]. However, to re-verify the accuracy of our developed DSMC solver, we simulate a pressure-driven microchannel flow and compare our results with available analytical solutions derived by imposing a second-order slip boundary condition [51]. The chosen 2D microchannel has  $8\text{ }\mu\text{m}$  length and  $0.4\text{ }\mu\text{m}$  height. The outlet is maintained at a pressure of 100 kPa, while the inlet/outlet pressures ratio is fixed at 2.0. This leads to a value of 0.141 for the outlet Knudsen number. Benefiting from a symmetric flow, we consider only one half of the channel in our simulation. The channel is divided into  $100 \times 30$  uniform cells, and a time step of

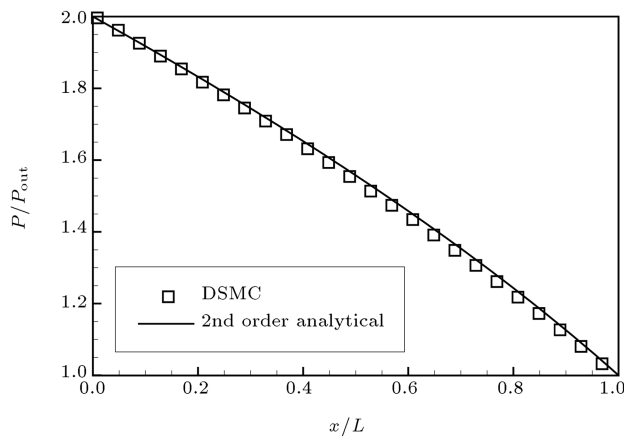


**Figure 1.** The results of developed DSMC solver for the centre-line pressure distribution of a pressure-driven microchannel flow and comparison with the analytical solution [51].

$1 \times 10^{-12}$  sec is used to perform the simulations. During the sampling period, i.e.  $8 \times 10^6$  time steps, or  $1.6 \times 10^6$  sampling steps, the average number of molecules is not less than 20 in each cell.

Figure 1 presents the pressure variations along the center-line of the microchannel. The analytical solution is also presented for comparison. It is observed that there is good agreement between the DSMC result and the analytical solution.

#### 4. Problem description

We simulate the mixing process of two parallel gas streams passing through nanomixers equipped with different throttle shapes, including a Linear Converging-Diverging throttle profile (LCD), an Arced Converging-Diverging throttle profile (ACD), and a Sudden Contraction-Expansion profile (SCE); see Figure 2. As is seen, these three mixer shapes have the same overall sizes. The nanomixer with no throttle is considered a basic mixer shape to compare our throttled mixing results with those of a blank mixer with no throttle. This blank mixer is depicted in Figure 2(a).

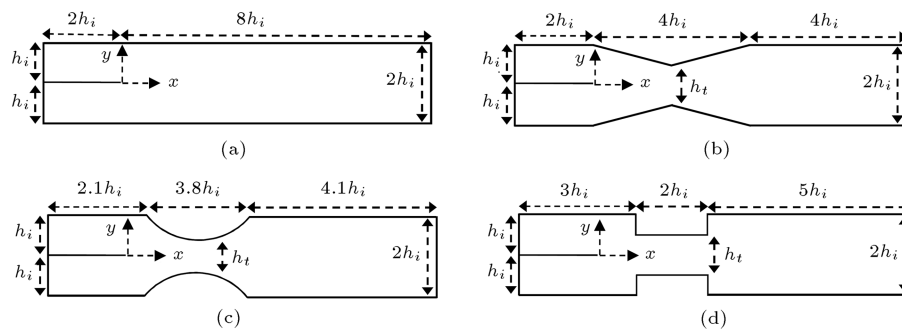


**Figure 2.** The schematics of basic nanomixer and the three nanomixers equipped with different throttle shapes but having equivalent overall sizes: (a) The basic (with no throttle) mixer profile; (b) Linear Converging-Diverging profile (LCD); (c) Arced Converging-Diverging profile (ACD); and (d) Sudden Contraction-Expansion (SCE).

We choose  $N_2$  and  $CO$  gases as our working fluids. Since these gases have the same molecular mass, the role of density is automatically eliminated in the study [3]. These two  $N_2$  and  $CO$  gas streams enter the nanomixer channel from the upper and lower inlets, respectively. All chosen nanomixers have an inlet width of  $h_i = 200$  nm. A splitter plate with a length of  $2h_i$  is used to separate the two incoming streams. In the next section, we investigate the effects of placing two different throttle widths,  $h_t = 1.0h_i$  and  $1.5h_i$ , in the mixing behaviour. Indeed, the nanomixer with no throttle can also be considered a basic shape, having a very specific throttle with a size of  $h_t = 2.0h_i$ .

Figure 2(b) shows a nanomixer with a Linear Converging-Diverging (LCD) throttle geometry/type. Certainly, this shape can be sufficient for studying the effect of throttle width on the performance of mixing. However, in addition to the width of the throttle, its shape may also influence fluid flow and mixing behaviours effectively. Therefore, we also incorporate the effect of throttle shape in our study, considering an Arced Converging-Diverging (ACD) throttle shape (Figure 2(c)), and a Sudden Contraction-Expansion (SCE) throttle shape (Figure 2(d)). Basically, these three throttle shapes have the same throttle width ( $h_t = h_i$ ) and mixer volume ( $V_m = 18h_i^2 \times 1$ ). As seen in Figure 2, all throttle centres are located at a distance of  $4h_i$  from the mixer inlet. To provide a better comparison between the three chosen geometries, Figure 3

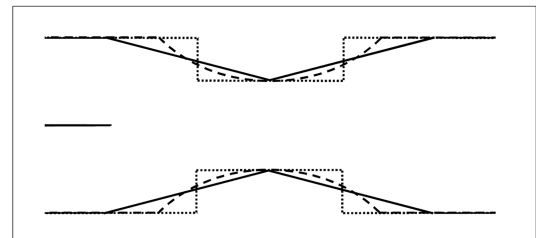


**Figure 3.** A close view of the contraction section of mixers with different throttle shapes. Solid line for the LCD profile, dashed line for the ACD profile, and dotted line for the SCE profile.

zooms in the throttle sections of LCD, ACD, and SCE mixers. Having different throttle profiles, we anticipate that they will effectively affect the mixing performance through and behind the throttle zone. The details are provided in the results and discussion section.

As the boundary condition implementations, we apply two pressures of 200 and 100 kPa at the inlet and outlet sections, respectively. Also, the inlet temperature and the wall temperatures are considered to be 300 K. The Knudsen number is estimated based on the inlet conditions for the  $N_2$  gas and using the inlet width, which is about 0.12. Therefore, the resulting flow would be in the transitional regime.

We use a structured grid of  $64 \times 40$  to perform our simulations for the LCD and ACD throttle configurations. The grid is non-uniform in the  $x$ -direction, so, the cells adjacent to the outlet section are 1.5 times more stretched in the  $x$ -direction than the cells adjacent to the inlet. In case of SCE configuration, we use the same cell sizes in the  $x$ -direction. However, we choose 40 and 80 cell divisions in the  $y$ -direction for the inner and outer regions of the throttle, respectively. A grid independency study for the basic nanomixer revealed that the selected grid sizes are fine enough for the current simulations; please see Section 5.1. The number of simulated molecules in each case is chosen in such a manner as to result in at least 20 molecules in each cell. The time step for the simulations is chosen to be  $5 \times 10^{-12}$  s.

## 5. Results and discussion

As described previously, we wish to investigate the effects of throttle width and shape on the mixing performance of the basic nanomixer, shown in Figure 2(a). In this regard, we first compare the achieved  $x$ -velocity distributions and the overall mass flow rate magnitudes of different nanomixers with each other and with those of the basic one. To evaluate the mixing performance, we also compare the resulting  $N_2$  mass fraction distributions and the achieved mixing length magnitudes of different mixers with each other. To quantify the mixing quality along the mixing channel, we use the relative density difference definition for the  $N_2$  gas. The relative density difference,  $\xi$ , is defined as [3]:

$$\xi(x) = 1 - \rho_0(x)/\rho_1(x). \quad (2)$$

In this work, we define the mixing length as an axial distance from the splitter end to the section at which  $\xi(x)$  reaches a value of 0.01.

### 5.1. Grid independence study

To ensure that the chosen computational grid of  $64 \times 40$  is fine enough and that it provides mesh-independent solutions for our DSMC simulations, we choose a finer

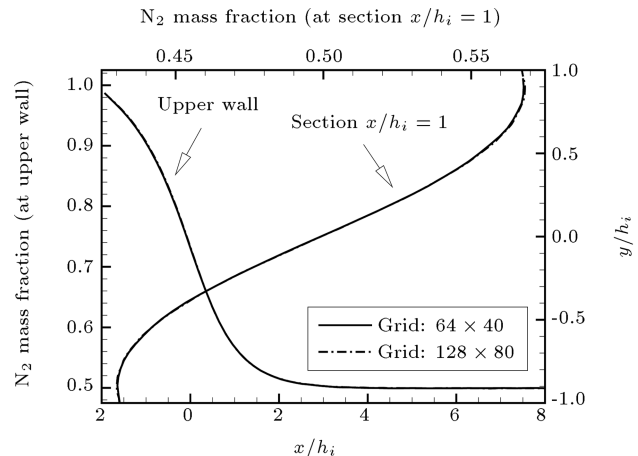


**Figure 4.** Distribution of  $N_2$  mass fraction along the upper wall of basic mixer and across section at  $x/h_i = 1.0$  using two different grid sizes.

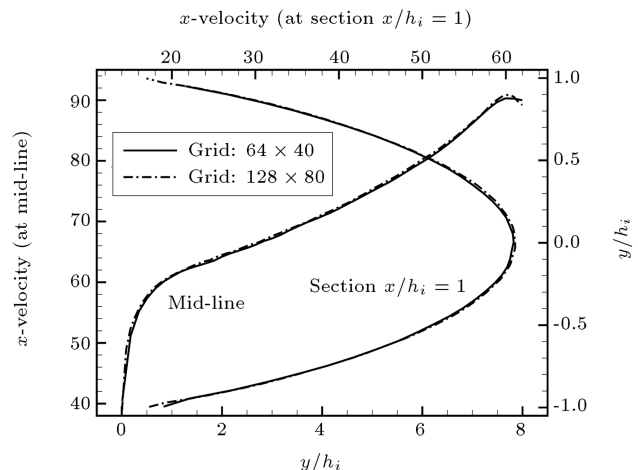


**Figure 5.** Distribution of  $x$ -velocity component along the centerline of basic mixer and across section  $x/h_i = 1.0$  using two different grid sizes.

grid of  $128 \times 80$  and simulate our base mixer, i.e. the nanomixer with no throttle (Figure 2(a)). Figure 4 presents the distribution of  $N_2$  mass fraction along the upper wall and also across a section located at  $0.2 \mu\text{m}$  downstream of the splitter, i.e. at  $x/h_i = 1$ . Figure 5 presents the variation of the  $x$ -velocity component along the mixer centre-line, starting from the splitter end. It also provides the  $x$ -velocity profile across the vertical section at  $x/h_i = 1$ . Figures 4 and 5 indicate that there are very slight differences between the results of two chosen grid sizes. In other words, a grid of  $64 \times 40$  would be fine enough to continue our current study.

### 5.2. Throttle width considerations

To study the effect of throttle width on mixer performance, we choose the LCD configuration and throttle widths of  $2.0h_i$ ,  $1.5h_i$  and  $1.0h_i$ . Figure 6 depicts the  $N_2$  mass fraction contours for three different LCD throttle widths of  $2.0h_i$ ,  $1.5h_i$  and  $1.0h_i$ . These plots show that

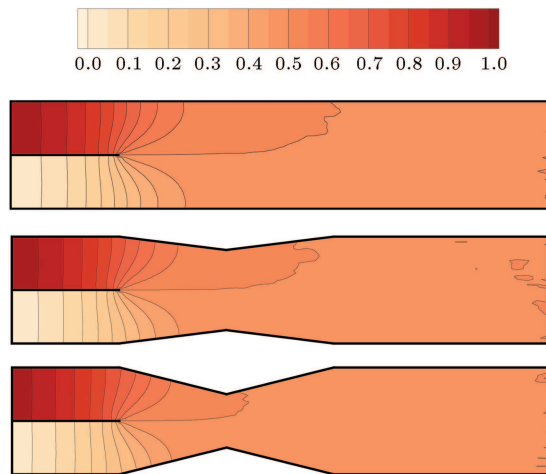


**Figure 6.** Contours of  $N_2$  mass fraction for the LCD mixer considering different throttle widths of  $2.0h_i$  (no throttle),  $1.5h_i$ , and  $1.0h_i$ .

the iso-mass fraction lines become more compressed at the inlets as the throttle width decreases. This means that full mixing would take place in a shorter length. It is also observed that the contour lines corresponding to  $Y_{N_2} = 0.5$  end at the upper wall and not the bottom wall. This means that the  $N_2$  gas would have smaller mass fraction values than those of CO in the resulting mixtures. Having the same molecular mass magnitudes, this occurrence is attributed to the small differences between the two gas VSS parameters, including the viscosity index ( $\omega$ ), the scattering exponent ( $\alpha$ ), and the reference diameter ( $d_{ref}$ ). If one follows Ref. [38] and uses its VSS parameters for  $N_2$  and CO gases, and the dynamics viscosity relations for the VSS collision model, one concludes that  $N_2$  viscosity is about 1.4% higher than CO viscosity at the temperature of 300 K. Therefore, the  $N_2$  gas stream experiences a little more resistance in the channels. This would cause the end of line  $Y_{N_2} = 0.5$  at the top wall.

Figure 7 presents the evolution of the relative density difference for the  $N_2$  gas, considering three different throttle widths:  $1.0h_i$ ,  $1.5h_i$  and  $2.0h_i$ . It is observed that the relative density difference performs a faster drop as the throttle width is gradually decreased. In other words, we expect a shorter mixing length as the throttle width decreases.

Choosing  $\xi = 0.01$  as our criterion to suppose a complete mixing process, the achieved mixing lengths will be  $2.01h_i$ ,  $2.56h_i$  and  $3.23h_i$  for the LCD mixer with throttle widths of  $1.0h_i$ ,  $1.5h_i$  and  $2.0h_i$ , respectively. This means that using throttle widths of  $1.0h_i$  and  $1.5h_i$  would, respectively, result in 38 and 21 percent reduction in mixing length compared to that of a blank mixer.

As can be predicted, if we reduce the passage width, it will result in a reduction in the diffusion

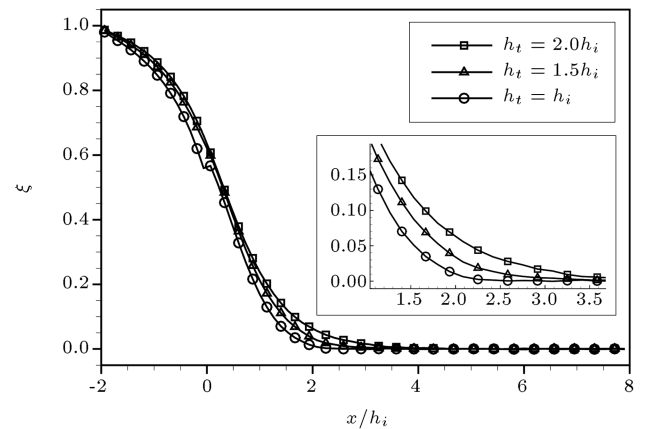


**Figure 7.** Evolution of relative density difference for LCD mixer considering different throttle widths of  $2.0h_i$ ,  $1.5h_i$  and  $1.0h_i$ .

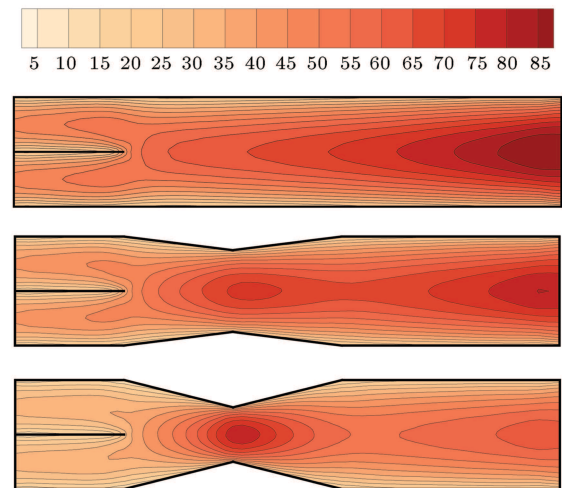


**Figure 8.** Contours of  $x$ -velocity (m/s) for the LCD mixer with different throttle widths of  $2.0h_i$  (no throttle),  $1.5h_i$  and  $1.0h_i$ .

distance or, equivalently, an increase in the concentration gradients. This would result in higher mass flux diffusion through the passage. So, this would automatically enhance the mixing performance. Figure 8 displays the  $x$ -velocity contours within the chosen LCD mixers. As seen, the fluid flow velocity increases more through a smaller throttle width if the outlet and inlet pressure conditions are fixed. Evidently, the velocity increase enhances the convective transport physics and limits the effects of concentration gradients. However, the achieved results indicate that the concentration gradient increase, which is a consequence of the throttle width decrease, would suffice to achieve a shorter mixing length.

Although flow velocity would normally increase at the throttle as the throttle width decreases, Figure 8 shows a reduction in velocity magnitude at the outlet section as the throttle width is decreased. So, this is an indication of mass flow rate reduction. The mass

flow rate through the nanomixers can be calculated by taking the integration over any arbitrary section across the mixing channel as follows:

$$\dot{m} = \int_{-h_i}^{+h_i} \rho u dy. \quad (3)$$

Taking this integration, we obtain the mass flow rates of  $2.28 \times 10^{-5}$ ,  $2.93 \times 10^{-5}$  and  $3.33 \times 10^{-5}$  kg/m.s for LCD mixers with throttle widths of  $1.0h_i$ ,  $1.5h_i$  and  $2.0h_i$ , respectively. In other words, the shapes with throttle widths of  $1.0h_i$  and  $1.5h_i$  reduce mass flow rate through the LCD nanomixer about 33 and 12 percent, respectively. Comparing the effects of throttle width on mixing length and mass flow rate, it is concluded that the mixing length is more sensitive than the mass flow rate value to throttle width magnitude.

### 5.3. Throttle shape considerations

To illustrate a quantitative study on the effects of throttle shape on the mixing performance, we choose the three LCD, ACD and SCE mixer configurations with the same overall sizes. Figure 9 presents the contours of  $N_2$  mass fractions within these three mixers. As observed, the contour lines in ACD and SCE shapes move more seriously towards the inlets than that of the LCD shape. This indicates that mixing would take place in shorter lengths using the ACD and SCE throttle shapes, although the effect is more pronounced for the SCE throttle.

Figure 10 presents the relative density difference variations along the mixer choosing the three LCD, ACD and SCE throttle shapes. We also present the relative density difference variation for the mixer with no throttle, in order to provide a good base to quantify our comparison. It is observed that the relative density difference is almost the same at the beginning of the mixing channel, i.e. at  $x/h_i = 0$ , for mixers with LCD and ACD throttles; although the ACD throttle performs a more rapid drop along the channel. Moreover,

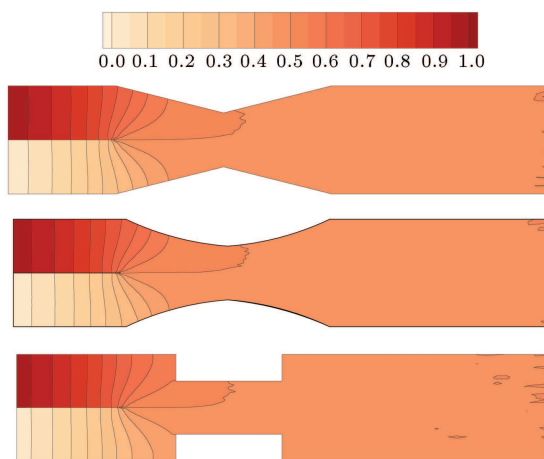


**Figure 9.** Contours of  $N_2$  mass fraction for the mixer equipped with different throttle shapes.

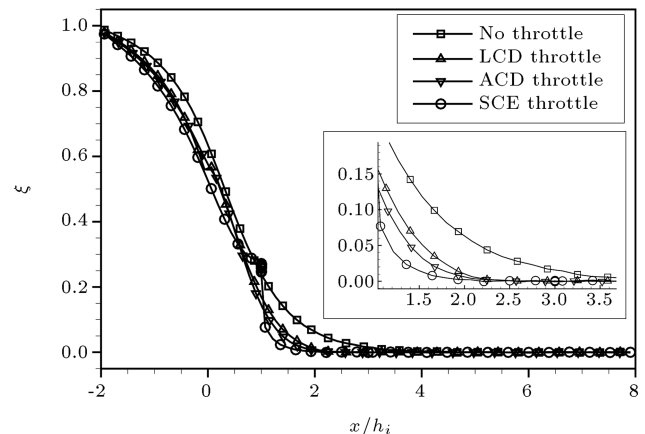


**Figure 10.** Evolution of relative density difference for the mixer equipped with different throttle shapes.

the mixer with a SCE throttle shows a lower value at the beginning of the mixing channel. It performs a slow drop until  $x/h_i = 1.0$ , which corresponds to the location of the sudden contraction. Compared with the case with no throttle, the SCE reaches a higher relative density difference value at  $x/h_i = 1.0$ . After this point, the relative density difference performs very abrupt drops and achieves values less than those obtained for other throttle shapes at the same sudden contraction section. Inspecting and evaluating the achieved relative density difference variations for the three chosen LCD, ACD and SCE mixers, we conclude that the LCD and SCE throttles would, respectively, result in the lowest and highest decreases in mixing length magnitude if compared with an equivalent mixer size with no throttle shape.

Choosing  $\xi = 0.01$  as a criterion to measure the mixing length, we arrive at  $2.01h_i$ ,  $1.88h_i$  and  $1.60h_i$  lengths for the nanomixers with LCD, ACD and SCE throttle shapes, respectively. Moreover, the mixing length would be equal to  $3.23h_i$  for the equivalent mixer with no throttle. These indicate that the LCD, ACD and SCE throttles with  $h_t = h_i$  would, respectively, result in about 38, 41 and 50 percent reductions in the achieved mixing length if compared with the mixing length of an equivalent mixer with no throttle.

Figure 11 presents the  $x$ -velocity component contours through the nanomixer applying different LCD, ACD and SCE throttle shapes. It is observed that using the ACD and SCE throttle shapes instead of LCD would generally reduce the velocity magnitudes through the nanomixer. The reduction is more pronounced in the case of using the SCE throttle shape.

Using Eq. (3), the mass flow rates are calculated as  $2.28 \times 10^{-5}$ ,  $2.09 \times 10^{-5}$  and  $1.73 \times 10^{-5}$  kg/m.s for mixers with LCD, ACD and SCE throttle shapes, respectively. As mentioned before, the mass flow rate would be  $3.33 \times 10^{-5}$  kg/m.s for the nanomixer with no throttle. This indicates that using the LCD, ACD



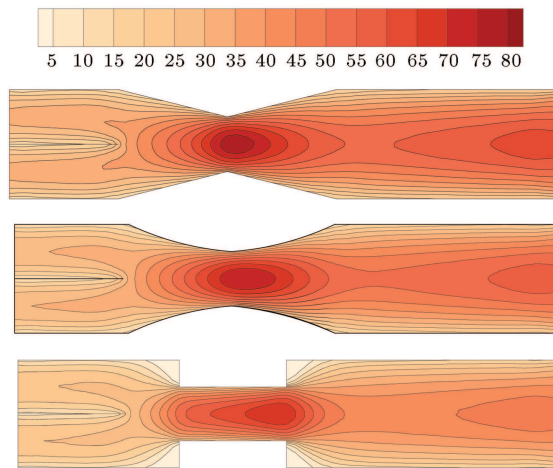


**Figure 11.** Contours of  $x$ -velocity (m/s) for the mixer equipped with different throttle shapes.

and SCE throttles with  $h_t = h_i$  would, respectively, result in about 32, 37, and 48 percent reductions in the mass flow rate through the mixer. So, appraising the effects of throttle shape on mixing length and mass flow rate magnitudes, one can readily conclude that throttle shape has a little more effect on mixing length than mass flow rate magnitude.

As was found, both flow passage width and flow velocity magnitude will affect the evolution of two parallel streams mixing through the mixing channel of a mixer. In the LCD and ACD throttle shapes, the flow passage widths will vary gradually along the mixing channel. However, the ACD throttle variation is more effective at the beginning of the throttle and this will result in a more serious blockage of the flow through the passage, see Figure 3. As seen in Figure 3, the ACD profile results in smaller passage widths (or, equivalently, shorter diffusion distances) and, consequently, higher species concentration gradients in the throttle region. On the other hand, a more effective blockage will result in a smaller velocity magnitude and, consequently, less mass flow rate through the nanomixer. Indeed, a higher concentration gradient and a smaller velocity magnitude would, mutually, tend to reduce mixing length. However, blockage effects and the reduction in diffusion distances are more pronounced for the case with the SCE throttle than in cases with LCD and ACD throttles. Therefore, if one chooses the SCE throttle shape, the mixing length and mass flow rate will reduce more effectively.

## 6. Conclusions

We investigate the effects of placing a throttle in the mixing channel of a gas nanomixer using the Direct Simulation Monte Carlo (DSMC) method. The study was performed at a Knudsen number of 0.12, which

takes into account the complexity of transitional flow regime influences, e.g. the slip phenomenon, in the mixing performance. At the first stage, our study shows that a decrease in the throttle width of a mixer with a linear converging-diverging contraction will result in a decrease in its mixing length. This reduction may be attributed to the enhancement of species concentration gradients, which is a direct consequence of reduction in flow passage width. The reduction in throttle width will also reduce the mass flow rate because of an increase in passage friction on the gas flow stream. Comparing the effects of throttle width on mixing length and mass flow rate magnitudes, it is observed that mixing length is more seriously affected by throttle width. At the second stage, we chose three different throttle shapes, including Linear Converging-Diverging (LCD), Arced Converging-Diverging (ACD), and Sudden Contraction-Expansion (SCE) throttle shapes, with equivalent overall sizes, to investigate the effects of throttle profile on mixing enhancement. Since the ACD profile causes a more serious flow passage blockage than the LCD profile, this, consequently, resulted in smaller mixing length and mass flow rate magnitudes for the mixer with the ACD throttle. On the other hand, since the SCE profile exhibits a greater flow blockage effect than the LCD and ACD profiles, this considerably reduces both its mixing length and mass flow rate magnitudes. Our conclusion is that throttle shape affects the mixing length value more considerably than mass flow rate magnitude through a nanomixer.

## Acknowledgment

The authors are grateful for the financial support received from the Deputy of Research and Technology at Sharif University of Technology, Tehran, Iran. It is greatly appreciated.

## Nomenclature

$h_i$	Mixer inlet width (nm)
$h_t$	Mixer throat width (nm)
$L$	Channel length ( $\mu\text{m}$ )
$\dot{m}$	Mass flow rate (kg/ms)
$u$	$x$ -velocity component (m/s)
$V_m$	Volume of nanomixer ( $\text{nm}^3$ )
$x, y$	Coordinates in longitudinal and transversal directions, respectively
$Y$	Species mass fraction
$\rho$	Total mass density of mixture ( $\text{kg/m}^3$ )
$\rho_0$	Mass density of $\text{N}_2$ gas, right near the bottom wall ( $\text{kg/m}^3$ )



$\rho_1$	Mass density of N <sub>2</sub> gas, right near the top wall (kg/m <sup>3</sup> )
$\xi$	Relative density difference

## References

1. Srinivasan, R., Hsing, I.-M., Berger, P.E., Jensen, K.F., Firebaugh, S.L., Schmidt, M.A., Harold, M.P., Lerou, J.J. and Ryley, J.F. "Micromachined reactors for catalytic partial oxidation reactions", *AIChE Journal*, **43**(11), pp. 3059-3069 (1997).
2. Xue, H., Yang, W., Chou, S.K., Shu, C. and Li, Z. "Microthermophotovoltaics power system for portable MEMS devices", *Microscale Thermophysical Engineering*, **9**(1), pp. 85-97 (2005).
3. Wang, M. and Li, Z. "Gas mixing in microchannels using the direct simulation Monte Carlo method", *International Journal of Heat and Mass Transfer*, **49**(9-10), pp. 1696-1702 (2006).
4. Le, M. and Hassan, I. "DSMC simulation of gas mixing in T-shape micromixer", *Applied Thermal Engineering*, **27**(14-15), pp. 2370-2377 (2007).
5. Adeosun, J.T. and Lawal, A. "Numerical and experimental mixing studies in a MEMS-based multilaminated/elongational flow micromixer", *Sensors and Actuators B: Chemical*, **139**(2), pp. 637-647 (2009).
6. Lee, J. and Kwon, S. "Mixing efficiency of a multilamination micromixer with consecutive recirculation zones", *Chemical Engineering Science*, **64**(6), pp. 1223-1231 (2009).
7. Ansari, M.A. and Kim, K.-Y. "Mixing performance of unbalanced split and recombine micromixers with circular and rhombic sub-channels", *Chemical Engineering Journal*, **162**(2) pp. 760-767 (2010).
8. Sheu, T.S., Chen, S.J. and Chen, J.J. "Mixing of a split and recombine micromixer with tapered curved microchannels", *Chemical Engineering Science*, **71**, pp. 321-332 (2012).
9. Jen, C.-P., Wu, C.-Y., Lin, Y.-C. and Wu, C.-Y. "Design and simulation of the micromixer with chaotic advection in twisted microchannels", *Lab on A Chip*, **3**(2), pp. 77-81 (2003).
10. Mouza, A.A., Patsa, C.-M. and Schönfeld, F. "Mixing performance of a chaotic micro-mixer", *Chemical Engineering Research and Design*, **86**(10), pp. 1128-1134 (2008).
11. Veenstra, T.T., Lammerink, T.S.J., Elwenspoek, M.C. and van den Berg, A. "Characterization method for a new diffusion mixer applicable in micro flow injection analysis systems", *Journal of Micromechanics and Microengineering*, **9**(2), pp. 199-202 (1999).
12. Gobby, D., Angeli, P. and Gavriilidis, A. "Mixing characteristics of T-type microfluidic mixers", *Journal of Micromechanics and Microengineering*, **11**(2), pp. 126-132 (2001).
13. Soleymani, A., Kolehmainen, E. and Turunen, I. "Numerical and experimental investigations of liquid mixing in T-type micromixers", *Chemical Engineering Journal*, **135**(1), pp. S219-S228 (2008).
14. Lee, M.G., Choi, S. and Park, J.-K. "Rapid multi-vortex mixing in an alternately formed contraction-expansion array microchannel", *Biomedical Microdevices*, **12**(6), pp. 1019-1026 (2010).
15. Kang, D.J., Song, C.M. and Song, D.J. "Junction contraction for a T-shaped micro-channel to enhance mixing", *Mechanics Research Communications*, **40**, pp. 63-68 (2012).
16. Wang, H., Iovenitti, P., Harvey, E. and Masood, S. "Optimizing layout of obstacles for enhanced mixing in microchannels", *Smart Materials and Structures*, **11**(5), pp. 662-667 (2002).
17. Bhagat, A.A.S., Peterson, E.T.K. and Papautsky, I. "A passive planar micromixer with obstructions for mixing at low Reynolds numbers", *Journal of Micromechanics and Microengineering*, **17**(5), pp. 1017-1024 (2007).
18. Alam, A., Afzal, A. and Kim, K.-Y. "Mixing performance of a planar micromixer with circular obstructions in a curved microchannel", *Chemical Engineering Research and Design*, **92**(3), pp. 423-434 (2014).
19. Pfeifer, P., Bohn, L., Görke, O., Haas-Santo, K., Schygulla, U. and Schubert, K. "Microstructured mixers for gas-phase processes - manufacture, characterization and applications", *Chemical Engineering & Technology*, **28**(4), pp. 439-445 (2005).
20. Shaker, M., Ghaedamini, H., Sasmito, A.P., Kurnia, J.C., Jangam, S.V. and Mujumdar, A.S. "Numerical investigation of laminar mass transport enhancement in heterogeneous gaseous microreactors", *Chemical Engineering and Processing: Process Intensification*, **54**, pp. 1-11 (2012).
21. Hsing, I.M., Srinivasan, R., Harold, M.P., Jensen, K.F. and Schmidt, M.A. "Simulation of micromachined chemical reactors for heterogeneous partial oxidation reactions", *Chemical Engineering Science*, **55**(1), pp. 3-13 (2000).
22. Yan, F. and Farouk, B. "Numerical simulation of gas flow and mixing in a microchannel using the direct simulation Monte Carlo method", *Microscale Thermophysical Engineering*, **6**(3), pp. 235-251 (2002).
23. Sasmito, A.P., Kurnia, J.C. and Mujumdar, A.S. "Numerical evaluation of transport phenomena in a T-junction microreactor with coils of different configurations", *Industrial & Engineering Chemistry Research*, **51**(4), pp. 1970-1980 (2012).
24. Reyhanian, M., Croizet, C. and Gatignol, R. "Numerical analysis of the mixing of two gases in a microchannel", *Mechanics & Industry*, **14**(6), pp. 453-460 (2013).
25. Zahmatkesh, I., Emdad, H. and Alishahi, M.M. "Navier-Stokes computation of some gas mixture problems in the slip flow regime", *Scientia Iranica, Trans-*

- actions *B: Mechanical Engineering*, **22**(1), pp. 187-195 (2015).
26. Kamali, R., Emdad, H. and Alishahi, M.M. "A new set of conservation equations based on the kinetic theory applied to gas mixture problems", *Scientia Iranica*, **14**(5), pp. 458-466 (2007).
  27. Kamali, R., Emdad, H. and Alishahi, M.M. "Multicomponent fluid flow analysis using a new set of conservation equations", *Fluid Dynamics Research*, **40**(5), pp. 343-363 (2008).
  28. Zahmatkesh, I., Emdad, H. and Alishahi, M.M. "Importance of molecular interaction description on the hydrodynamics of gas mixtures", *Scientia Iranica Transactions B: Mechanical Engineering*, **18**(6), pp. 1287-1296 (2011).
  29. Zahmatkesh, I., Emdad, H. and Alishahi, M.M. "Two-fluid analysis of a gas mixing problem", *Scientia Iranica Transactions B: Mechanical Engineering*, **20**(1), pp. 162-171 (2013).
  30. Hadjiconstantinou, N. "Comment on Cercignani's second-order slip coefficient", *Physics of Fluids*, **15**(8), pp. 2352-2354 (2003).
  31. Lockerby, D.A., Reese, J.M., Emerson, D.R. and Barber, R.W. "Velocity boundary condition at solid walls in rarefied gas calculations", *Physical Review E*, **70**(1), p. 017303 (2004).
  32. Roohi, E. and Darbandi, M. "Extending the Navier-Stokes solutions to transition regime in two-dimensional micro- and nanochannel flows using information preservation scheme", *Physics of Fluids*, **21**(8), p. 082001 (2009).
  33. Darbandi, M. and Vakilipour, S. "Solution of thermally developing zone in short micro/nanoscale channels", *Journal of Heat Transfer*, **131**(4), p. 044501 (2009).
  34. Vakilipour, S. and Darbandi, M. "Advancement in numerical study of gas flow and heat transfer in microchannel", *Journal of Thermophysics and Heat Transfer*, **23**(1), pp. 205-208 (2009).
  35. Le, N.T.P., White, C., Reese, J.M. and Myong, R.S. "Langmuir-Maxwell and Langmuir-Smoluchowski boundary conditions for thermal gas flow simulations in hypersonic aerodynamics", *International Journal of Heat and Mass Transfer*, **55**(19-20), pp. 5032-5043 (2012).
  36. Qazi Zade, A., Renksizbulut, M. and Friedman, J. "Slip/jump boundary conditions for rarefied reacting/non-reacting multi-component gaseous flows", *International Journal of Heat and Mass Transfer*, **51**(21-22), pp. 5063-5071 (2008).
  37. Qazi Zade, A., Ahmadzadegan, A. and Renksizbulut, M. "A detailed comparison between Navier-Stokes and DSMC simulations of multicomponent gaseous flow in microchannels", *International Journal of Heat and Mass Transfer*, **55**(17-18), pp. 4673-4681 (2012).
  38. Bird, G.A., *Molecular gas dynamics and direct simulation of gas flows*, Oxford University Press, Oxford, UK (1994).
  39. Wang, M. and Li, Z. "Simulations for gas flows in microgeometries using the direct simulation Monte Carlo method", *International Journal of Heat and Fluid Flow*, **25**(6), pp. 975-985 (2004).
  40. Roohi, E., Darbandi, M. and Mirjalili, V. "Direct simulation Monte Carlo solution of subsonic flow through micro/nanoscale channels", *Journal of Heat Transfer*, **131**(9), p. 092402 (2009).
  41. Gatsonis, N.A., Al-Kouz, W.G. and Chamberlin, R.E. "Investigation of rarefied supersonic flows into rectangular nanochannels using a three-dimensional direct simulation Monte Carlo method", *Physics of Fluids*, **22**(3), p. 032001 (2010).
  42. Darbandi, M. and Roohi, E. "Study of subsonic-supersonic gas flow through micro/nanoscale nozzles using unstructured DSMC solver", *Microfluidics and Nanofluidics*, **10**(2), pp. 321-335 (2011).
  43. Darbandi, M. and Roohi, E. "DSMC simulation of subsonic flow through nanochannels and micro/nano backward-facing steps", *International Communications in Heat and Mass Transfer*, **38**(10), pp. 1443-1448 (2011).
  44. Roohi, E. and Darbandi, M. "Recommendations on performance of parallel DSMC algorithm in solving subsonic nanoflows", *Applied Mathematical Modeling*, **36**(5), pp. 2314-2321 (2012).
  45. Darbandi, M. and Roohi, E. "A hybrid DSMC/Navier-Stokes frame to solve mixed rarefied/non-rarefied hypersonic flows over micro/nano obstacles", *International Journal for Numerical Methods in Fluids*, **72**(9), pp. 937-966 (2013).
  46. Darbandi, M. and Roohi, E. "Applying a hybrid DSMC/Navier-Stokes frame to explore the effect of splitter catalyst plates in micro/nanopropulsion systems", *Sensors and Actuators A: Physical*, **189**, pp. 409-419 (2013).
  47. Ejtehadi, O., Roohi, E. and Abolfazli Esfahani, J. "Detailed investigation of hydrodynamics and thermal behavior of nano/micro shear driven flow using DSMC", *Scientia Iranica, Transactions B: Mechanical Engineering*, **20**(4), pp. 1228-1240 (2013).
  48. Moríño, J.A. and Hermida-Quesada, J. "Solid-gas surface effect on the performance of a MEMS-class nozzle for micropropulsion", *Sensors and Actuators A: Physical*, **162**(1), pp. 61-71 (2010).
  49. La Torre, F., Kenjeres, S., Kleijn, C.R. and Moerel, P.A. "Effects of wavy surface roughness on the performance of micronozzles", *Journal of Propulsion and Power*, **26**(4), pp. 655-662 (2010).
  50. Scanlon, T.J., Roohi, E., White, C., Darbandi, M. and Reese, J.M. "An open source parallel DSMC code for rarefied gas flows in arbitrary geometries", *Computers & Fluids*, **39**(10), pp. 2078-2089 (2010).
  51. Karniadakis, G., Beskok, A. and Aluru, N.R., *Microflows and Nanoflows Fundamentals and Simulation*, Springer, New York (2005).

## Biographies

**Masoud Darbandi** received BS (1986) and MS (1989) degrees from Sharif University of Technology (SUT), Tehran, Iran, and his PhD degree in computational fluid dynamics from the University of Waterloo (UW), Canada, in 1996. He is currently Professor in the Aerospace Engineering Department of Sharif University of Technology (SUT), Tehran, Iran, and Adjunct Professor at the Institute for Nanoscience and Nanotechnology. His research interests include CFD, nanoscale, microscale, and continuous fluid flow simulations using molecular, mesoscopic and continuum- and semi-continuum based methods. He has also been

active in many industrial projects engaged with energy production, energy conversion, energy consumption, and their optimization.

**Moslem Sabouri** received BS and MS degrees in Aerospace Engineering in 2007 and 2009, respectively, from Sharif University of Technology (SUT), Tehran, Iran, where he is currently a PhD candidate. His research interests include micro/nanoscale flow simulations using CFD, DSMC, MD, and hybrid methods. This paper is part of his PhD research work entitled, “Developing a hybrid continuum-molecular method to analyze binary gas mixing and separation processes”, supervised by Prof. M. Darbandi.